BMC Infectious Diseases

CASE REPORT

Open Access

Respiratory microbiome alterations, coinfections and virus intra-host evolution in a persistently active SARS-CoV-2 infection

Lučka Boltežar[1,5], Rok Kogoj[2], Katarina Resman Rus[2], Alen Suljič[2], Martin Bosilj[2], Nataša Knap[2], Polonca Mali[3], Janez Tomažič[4,5], Tatjana Avšič-Županc[2] and Misa Korva[2*]

Abstract

Background Respiratory microbiome alterations, coinfections, and virus intrahost evolution are of great interest in persistently viable SARS-CoV-2 infections in the context of antiviral treatment and immune response. However, samples before, during, and after infection are seldom available to researchers. Therefore, there has been a significant lack of opportunities to comprehensively study microbiota homeostasis, coinfections, and virus intra-host evolution on the consensus and minor variants scale in response to antiviral treatments and patient immune response.

Case presentation A 63-year-old female patient with diffuse large B-cell lymphoma received multiple treatments for SARS-CoV-2 that remained active 169 days. Together, 32 respiratory and 19 serum samples were collected before, during, and after (− 398 to 233 days) COVID-19. Subsets were selected for virus viability testing by culture (20) and subgenomic (sg) RNA (20) measurement, intra-host evolution assessment (18), microbiome composition analysis (28), and coinfection identification (11). IgA/IgG and neutralizing anti-SARS-CoV-2 antibodies were measured 19 times throughout the infection. SARSCoV-2 lineage XBB.1.16.11 persisted and remained viable until 116 days post infection (PI) regardless of treatments. No sgRNA marker tested was suitable for virus viability prediction. IgG/IgA antibodies first appeared after 38 days, but the virus persisted regardless of multiple plasma treatments before neutralizing antibodies appeared (100 days PI) and finally cleared the virus 116 days PI. Consensus-level mutations fluctuated around 102.7 ± 4.0, and minor variants increased from six to 61 with a mutation rate of 4.9×10^{-3} per site per year, with the highest average number of mutations per gene length in S and E (0.013) with surges after every antiviral treatment. The transversion/transition ratio increased from 0.50 (day 0) to 0.57 (day 24) with a steady decrease to 0.48 (day 147). Mutational signature analysis showed dominance of C > T substitutions consistent with APOBEC antiviral enzyme activity. Upper respiratory microbiota showed three distinct profiles with varying α-/β-diversity and an association of *Staphylococcus* spp. with COVID-19.

Conclusions These findings further elucidate the dynamics of intra-host viral evolution and complexities of virus clearance in individuals with hematological malignancies and highlight the impact of antiviral treatments on the potential of virus variants emergence in longitudinally infectious patients due to delayed immune response.

*Correspondence:
Misa Korva
misa.korva@mf.uni-lj.si

Full list of author information is available at the end of the article

Keywords Microbiome, Prolonged SARS-CoV-2 infection, Virus evolution, Virus shedding, Hematological malignancies, B-cell lymphoma

Background

Individuals with hematological malignancies remain particularly vulnerable to SARSCoV-2–associated morbidity and mortality due to their underlying disease, which limits prevention strategies, treatment, and elimination of the virus [1]. It has been shown that such patients can be an important source for the evolution of the virus [2]; however, less is known about whether the SARS-CoV-2 lineage remains the same [3], how long viral infectivity is retained [4], and how antiviral therapy impacts viral evolution [5]. Understanding the effect of multiple antiviral treatments on the potential for new virus variant emergence (virus mutagenesis) in the context of infectivity longevity, disease progression, and clearance of SARS-CoV-2 in these cases is therefore of utmost importance for developing better patient management strategies and refining infection prevention guidelines.

Case presentation

A 63-year-old female patient with advanced-stage follicular lymphoma that had transformed into diffuse large B-cell lymphoma with lymph node involvement above and below the diaphragm was regularly screened for SARS-CoV-2 infection. The patient received three types of systemic treatment, including rituximab, and radiotherapy encompassing almost the entire abdomen with the aim of CAR-T therapy. However, during the course of her anti-cancer treatment (Supplement), the patient developed severe myopathy and was infected with SARS-CoV-2. Initially, the patient received multiple courses of remdesivir and convalescent plasma (CCP) for treatment of the SARS-CoV-2 infection. The total number of CCP units administered was 28, amounting to approximately 6.5 l (two units of CCP were transfused upon each treatment). Due to SARS-CoV-2 persistence, the therapeutic approach was modified by adding nirmatrelvir/ritonavir. Antiviral treatment was terminated on day 130 post infection (PI), when the patient was SARS-CoV-2 negative for the first time after 4 months. However, the emergence of recurrent fever on day 147 PI prompted further SARSCoV-2 testing, which was positive (Ct = 20). The patient was then re-treated with a combined therapy until she was finally SARS-CoV-2 negative from day 171 PI onward.

During SARS-CoV-2 infection, the patient was continuously treated for the underlying disease, and while she was in the hospital she acquired multiple additional infections. Voriconazole and anidulafungin were administered due to lung aspergillosis and fungal sepsis, pneumonia caused by *Klebsiella pneumoniae* was treated with meropenem, anogenital herpes was treated with valacyclovir, ganciclovir was used for CMV reactivation, cefuroxime was administered for a urinary tract infection with *K. pneumoniae*, and *Staphylococcus* spp. sepsis was addressed with vancomycin.

Nasopharyngeal, sputum, and serum samples were collected before, during, and after SARS-CoV-2 infection (– 398 to 233 days). Subsets of samples were selected for virus viability testing by cell culture (20 samples) and subgenomic (sg) RNA detection (21 samples), investigation of intra-host evolution (18 samples), respiratory microbiome interaction determination (28 samples), coinfection identification (11 samples), and the patient's immune response analysis (19 samples; Table 1). Methodology details are presented in Supplement.

Virus culture confirmed SARS-CoV-2 viability until day 24 PI. The initial unsuccessful virus rescue in Vero E6 cells (days 38, 43, and 50 PI) coincides with the onset of seroconversion, as evidenced by the detection of IgG and IgA antibodies in the patient's serum. In fact, IgA antibodies already started to increase between days 10 and 16 PI from total absence to just under the borderline region (≥ 0.8 to < 1.1), suggesting that, although immunocompromised, the patient developed an antibody response in spite of only recently terminated rituximab treatment, which is consistent with previous findings [6, 7]. Viable virus was later again detected from day 59 PI to day 116 PI. Subsequently, receiving plasma with a high neutralization titer (1:640–320) over 54 days resulted in a neutralizing response that finally neutralized the infectious virus from day 126 PI onward (Fig. 1). The relative abundance of SARS-CoV-2 sgRNA to gRNA was stable over time and did not correlate with viable virus (Fig. 1). However, an increasing agreement between the respective molecular marker and viable virus was observed for genomic RNA (65.0%), subgenomic N gene RNA (70.6%), and subgenomic M gene RNA (80.0%; Table 2).

Good sequencing data with a 99.53% ± 0.42% (min: 98.53%, max: 99.76%) coverage of the SARS-CoV-2 genome was obtained for 15 samples included. Samples collected on days 66, 162, and 169 PI showed only ≤ 75% genome coverage and were therefore excluded from further analysis. In the consensus sequences, only lineage XBB.1.16.11 with a relatively stable number of nucleotide mutations was detected throughout the infection. To exclude a reinfection, whole genome phylogenetic analysis was performed, which confirmed intra-host evolution of the virus as seen by distinct branching of the patient's sequences in comparison to the local population from the time of infection onward (Supplement). A median of

Table 1 Timeline of clinical samples collected with results

Days PI	Sample no.	Sample type	rtRT-PCR		Virus viability: CPE/logTCID$_{50}$/ml	Serology			Sequencing		
			gRNA	sgRNA (N/M)		IgG[†]	IgA[†]	NT	Variants	16 S meta	Coinfections
−398	1	NP	NEG	—	—				—	YES	
−377	2	NP	NEG	—	—				—	YES	
−135	3	NP	NEG	—	—				—	YES	
−73	4	NP	NEG	—	—				—	YES	
−39	5	NP	NEG	—	—				—	YES	
−18	6	NP	NEG	—	—				—	YES	
0	7	NP	19.78	32.7/35.1	—				YES	YES	
5	S1	Serum				0.10	0.09	NEG			
10	S2	Serum				0.10	0.10	NEG			
11	8	NP	12.64	24.0/27.3	YES/8.88				YES	YES	YES
16	S3	Serum				0.43	0.78	NEG			
17	9	NP	14.56	27.3/25.9	YES/8.75				YES	YES	YES
	9a	Sputum									YES
24	10	NP	14.37	25.9/28.4	YES/6.88				YES	YES	
38	S4, 11	Serum and NP	16.80	26.3/29.5	NEG	2.00	1.87	NEG	YES	YES	
43	S5, 12	Serum and NP	16.22	23.6/27.3	NEG	4.72	5.07	NEG	YES	YES	
50	13	NP	20.33	28.7/32.1	NEG				YES	YES	
51	S6	Serum				2.94	1.74	NEG			
59	S7, 14	Serum and NP	12.92	23.2/27.2	YES/8.75	5.76	7.85	NEG	YES	YES	
60	S8	Serum				5.77	7.13	NEG			
66	15	NP	14.25	—	—				YES	YES	
71	S9, 16	Serum and NP	12.95	24.8/27.8	YES/8.88	6.60	8.15	NEG	YES	YES	
78	17	NP	13.97	23.8/27.0	YES/7.63				YES	YES	
93	18	NP	11.99	25.2/29.4	YES/7.88				YES	YES	YES
94	S10	Serum				6.63	2.88	NEG			
95	18a	Sputum									YES
100	S11	Serum				7.53	7.50	1:10			
101	19	NP	26.35	36.8/NEG	YES/6.25				YES	YES	
116	S12, 20	Serum and NP	16.43	26.9/31.5	YES/6.75	8.16	5.32	1:10	YES	YES	YES
126	21	NP	32.22	NEG/NEG	NEG				YES	YES	
130	22	NP	NEG	NEG/NEG	NEG				—	YES	
134	S13	Serum				9.47	5.38	1:20			
144	S14, 23	Serum and NP	NEG	NEG/NEG	NEG	6.87	2.35	1:10	—	YES	YES
147	24	NP	20.52	33.1/NEG	NEG				YES	YES	YES
148	S15	Serum				7.44	1.52	1:10			
159	S16	Serum				6.74	4.74	1:20			
162	25	NP	26.17	38.4/NEG	NEG				YES	YES	YES
166	S17	Serum				6.82	4.74	1:10			
169	26	NP	31.89	NEG/NEG	NEG				YES	YES	YES
	26a	Sputum									YES
171	S18, 27	Serum and NP	NEG	NEG/NEG	NEG	8.47	2.82	1:10	—	YES	
179	28	NP	NEG	NEG/NEG	NEG				—	YES	
212	29	NP	NEG	—	—				—	—	
233	S19	Serum				3.88	0.22	NEG			

[†]= target antigen: S1 domain of the SARS-CoV-2 spike (S) protein. Cutoff value: negative < 0.8 and positive > 1.1; NT = neutralization assay result; NP = nasopharyngeal swab

102.7 ± 4.0 (min: 98, max: 116) mutations compared to the Wuhan HU-1 (GeneBank: NC_045512.2) strain was observed. The calculated mutation rate based on linear regression analysis was 5.5×10^{-4} per site per year. On the minor variant scale, the number of mutations steadily increased over time, with a mutation rate of 4.9×10^{-3} per site per year, with the highest calculated average number of mutations/gene length in E (0.013; min 0.009– max 0.018) and S (0.013; min 0.012– max 0.019). We observed a shift in favor of transversions from the beginning of infection until day 30 PI and then a gradual return to a ratio below 0.5. This observation does not directly

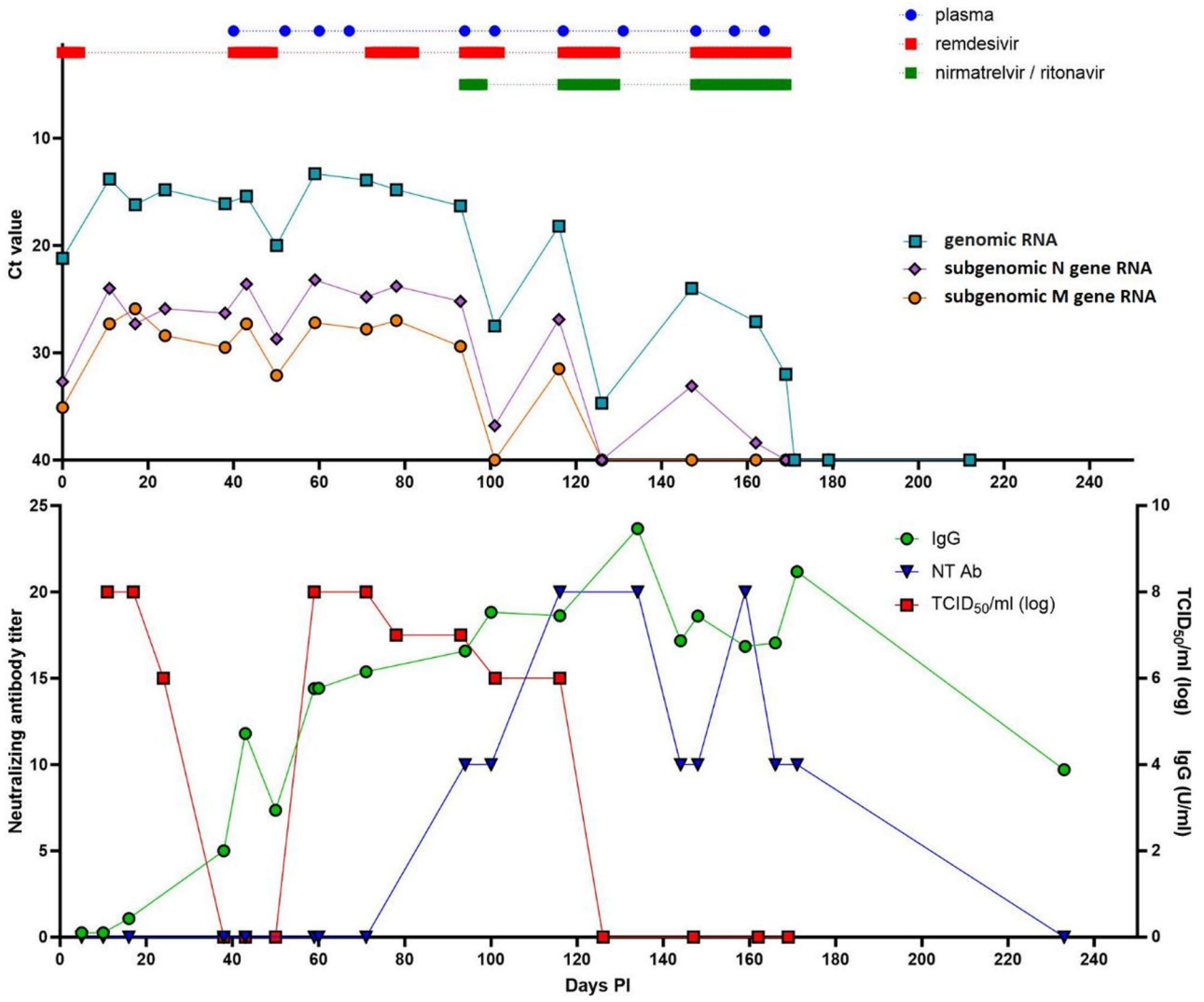

Fig. 1 Composite graph showing the timeline of antiviral therapy type and administration strategy with corresponding genomic and subgenomic rtRT-PCR results and correlation with $TCID_{50}$/ml, neutralizing antibody, and IgG antibody quantities

Table 2 2×2 comparison of agreement between virus isolation and genomic and subgenomic N gene and M gene RNA detection

		Genomic RNA		Subgenomic RNA marker			
				N gene		M gene	
		POS	NEG	POS	NEG	POS	NEG
Virus isolation	POS	9	0	9	0	8	1
	NEG	7	4	5	6	3	8
Agreement [%]		65.0% (95CI: 43.3–81.9%)		70.6% (95CI: 53.1–88.8%)		80.0% (95CI: 58.4 – 91.9%)	

translate into the temporal dynamics of the Syn/nSyn mutation ratio, which fluctuated but always remained in favor of nSyn. In total, 131 distinct consensus-level mutations were identified, 99 of which were present across all samples (mutual mutations), whereas 32 sporadically occurred (fluctuating mutations). Among the 99 mutual mutations, 60 were lineage defining, and the remaining 39 less frequently occur in lineage XBB.1.16.11. Among the 32 fluctuating mutations, only three were lineage defining. Deletions in the genome were also observed, but it remained stable at 44 and did not change through the progression of infection. A high number of minor-level SNPs fluctuated between consensus-level frequencies (50%) and sequencing errors (5%) [8, 9]. Such a dynamic is indicative of viral evolution during infection, despite no changes in the consensus. This is further supported by

the temporal and positional analysis of nucleotide mutations on the minor variant scale, which revealed that until day 71 PI there was a slow yet gradual increase up to 15 non-synonymous and fewer than 10 synonymous nucleotide mutations. After day 71 PI, however, a quick surge to more than 45 non-synonymous and 17 synonymous minor scale mutations with a later drop back to similar numbers before this event was observed. Interestingly, no apparent hotspots could be detected, neither on the minor or major variant scale, with the highest average number of mutations/gene length in ITR (0.06), followed by S and E (both 0.013). However, it is noteworthy that, although only minor changes in the virus were observed on the major variant scale, surges in the number of mutations on the minor scale coincide with every round of antiviral treatment (Fig. 2). Three mutations in the nsp12 gene associated with remdesivir treatment, but not necessarily resistance, were observed. The G617S mutation

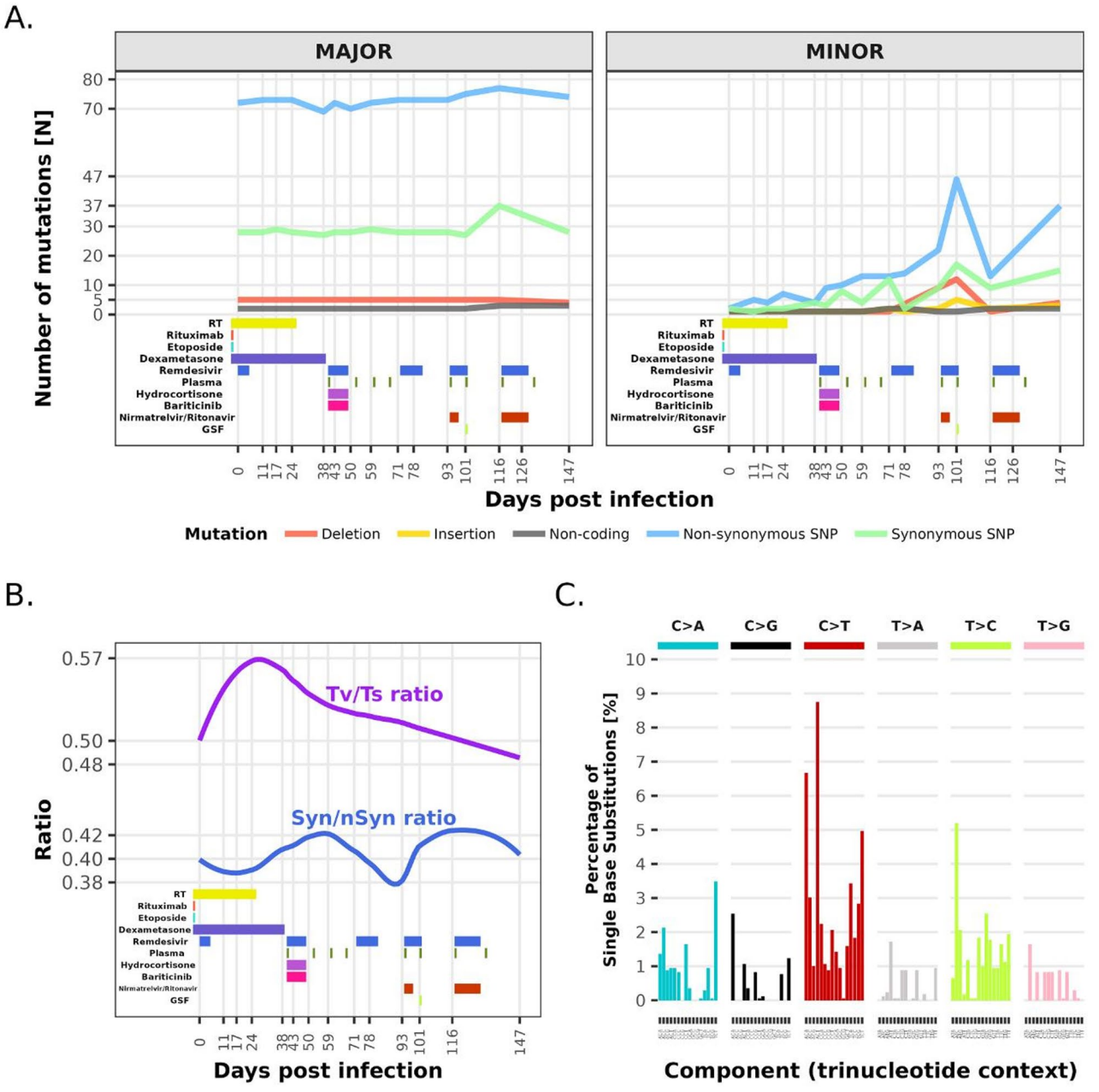

Fig. 2 **A** Accumulation of mutations (*n*) on the major and minor variant level against the reference Wuhan Hu-1 strain (GeneBank: NC_045512.2) in relation to underlying disease and antiviral treatment. **B** Ratio between transversions versus transitions (Tv/Ts) and synonymous versus non-synonymous mutations (Syn/nSyn) in relation to days PI and underlying disease and antiviral treatment. **C** Single base substitution (SBS)–96 mutational signatures derived from 17 sequenced samples

was present at a fixed major level (frequency: ~100%) in all samples, whereas the V792I mutation occurred at a minor level (frequency: ~5%) on day 147. On the other hand, the A449V mutation, initially observed at a minor level on days 59 and 93 (frequency: ~5%), showed a transient increase on day 116 (frequency: ~26%), followed by a renewed decrease on day 147 (frequency: ~14%). No other mutations known to be implicated in remdesivir resistance, or mutations in the nsp5 gene linked to reduced susceptibility to nirmatrelvir, were observed on either the minor or major scale.

Upper respiratory microbiome analysis revealed a higher α-diversity (Shannon entropy) for phases before and post SARS-CoV-2 infection. The difference between before and during SARS-CoV-2 infection was also statistically significant (pairwise Kruskal–Wallis test; $p = 0.02$). β-diversity showed a higher dispersion in phase 2 than in phases 1 and 3. The genus *Staphylococcus* was significantly associated with phase 2 (*W*-score: 89; Fig. 3).

The NGS approach for detection of respiratory pathogens and antibiotic resistance genes identified some of the pathogens in earlier samples than targeted testing. Interestingly, NGS showed rhinovirus A to be present in the patient samples throughout the time of the SARSCoV-2 infection. Based on reads classification results, Rhinovirus A2 strain USA/2018/CA-RGDS-1062

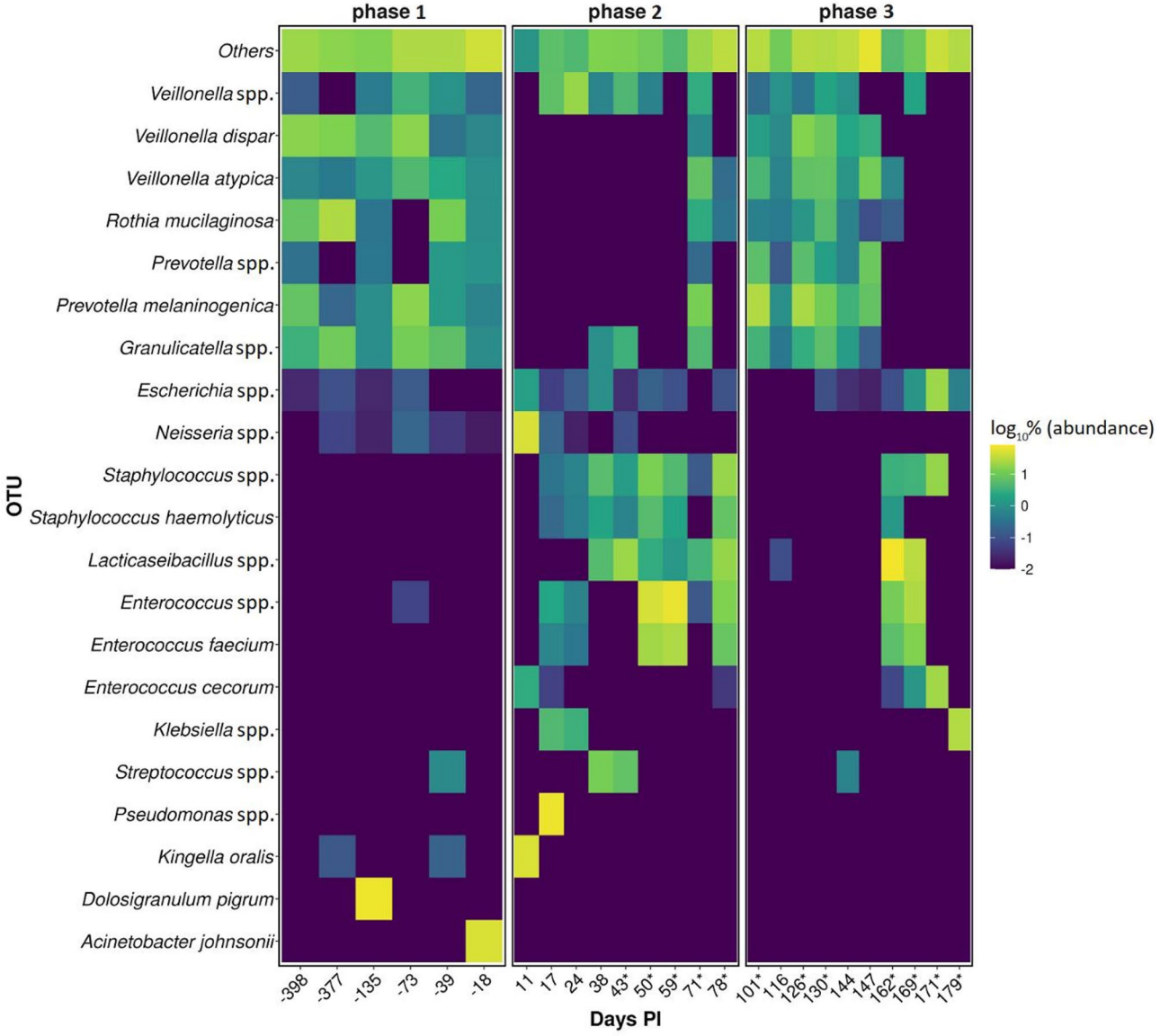

Fig. 3 Heatmap showing the 21 most abundant bacterial operational taxonomic units (OTUs) (*y*-axis) per day PI (*x*-axis). The remaining species detected are grouped in one category (Others). Each of the three phases represents samples according to SARS-CoV-2 infection status. The color of each box corresponds to the relative abundance of respective bacterial species as $\log_{10}$%. If a box is not visible, the species was not detected in the respective sample; * marks days on which a specific antiviral treatment was administered

Table 3 Coinfection detection using the respiratory pathogen ID panel showing known and potentially pathogenic microorganism hits with detected AMR genes

Sample no.	Days PI	Detected pathogen with conventional methods	Detected pathogen using NGS	AMR gene (% identity)
8	11	SARS-CoV-2	SARS-CoV-2/Rhinovirus A	N/A
9	17	SARS-CoV-2	SARS-CoV-2/Rhinovirus A/*K. pneumoniae*/*E. faecium*	blaTEM-1 (100)
9a		*K. pneumoniae*/*C. albicans*/*C. krusei*/*A. fumigatus*	SARS-CoV-2/*K. pneumoniae*/*A. fumigatus*	N/A
18	93	SARS-CoV-2/Rhinovirus	SARS-CoV-2/Rhinovirus A/*A. flavus*	N/A
18a	95	*K. pneumoniae*/*C. krusei*	SARS-CoV-2/Rhinovirus A/*K. pneumoniae*/*S. mitis*/*S. odontolytica*	erm(B) (100), erm(X) (100)
20	116	*K. pneumoniae* in urine	SARS-CoV-2/Rhinovirus A/*K. pneumoniae*/*S. mitis*/*S. odontolytica*/*G. haemolysans*	erm(B) (100)
23	144	*K. pneumoniae* in urine	SARS-CoV-2/*K. pneumoniae*/*S. mitis*/*S. odontolytica*/*G. haemolysins*/*S. aureus*/*N. meningitidis*	erm(B) (100), vga(A) (97.32)
24	147	SARS-CoV-2/Rhinovirus	SARS-CoV-2/Rhinovirus A/*S. odontolytica*/*N. meningitidis*	erm(B) (99.87)
25	162	SARS-CoV-2	SARS-CoV-2/*E. faecium*/	ant(6)-Ia (100), erm(B) (99.87), mph(C) (84.11), msr(C) (100)
26	169	SARS-CoV-2	SARS-CoV-2/Rhinovirus A/*E. faecium*	aph(3')-IIIa (100), erm(B) (99.87), erm(C) (96.33), mecA (100), msr(C) (96.15), tet(M) (100)
26a		*E. faecium*/*C. krusei*	SARS-CoV-2/Rhinovirus A/*E. faecium*	ant(6)-Ia (99.89), msr(C) (100)

(GeneBank: MN228695.1) was consistently detected in all samples with the highest classification scores, thus pointing to a single chronic infection rather than multiple distinct infections. Furthermore, the detected amount and spectrum of present antimicrobial resistance (AMR) genes gradually increased; however, the detected resistance genes cannot be directly linked to bacteria identified as etiologically important. Moreover, infections with *K. pneumoniae*, *Staphylococcus* spp., and *E. faecium* were not treated with the antibiotics against which potential resistance was molecularly detected (Table 3).

Discussion

There are no guidelines and recommendations for optimal strategies in managing persistent SARS-CoV-2 infection in patients with B-cell lymphoma. Often, the standard antiviral monotherapy regimen, initially validated for treatment of COVID-19 immunocompetent patients, proves ineffective [10]. Monotherapy is likely to drive the emergence of treatment-related immune escape, relapses, and delayed treatment of the underlying disease [11]. An off-label treatment approach to mitigate such consequences is therefore based on combination therapies [12]. Similar to the report from Mendes-Correa et al. [13], we demonstrated sustained SARS-CoV-2 replicative capacity for more than 116 days PI. During the infection, the virus culture was negative only between days 38 and 50 PI. We believe that both antiviral treatment and the patient's immune response significantly reduced the quantity of infectious virus and influenced the viral mutations—and this, in turn, likely led to virus concentrations falling below the threshold necessary for successful in vitro isolation. This is supported by previous findings showing that virus culture systems, particularly those using Vero E6 cells, have limited sensitivity [13, 14]. Such a limitation of the in vitro system is consistent with findings in Ebola virus rescue from semen samples, for which viral viability could not be confirmed in cells but could be demonstrated in SCID mice [15]. The fact that the patient did not infect any family members further supports the idea that there were low concentrations of infectious virus. Reinfection was ruled out by phylogenetic analysis and data from the national SARS-CoV-2 lineage monitoring program because no cases of XBB.1.16.11 were detected in the general population at that time. Nevertheless, the virus remained viable in vivo, as reflected by the emergence of nsp12 mutations (A449V, G671S, and V792I), which are associated with remdesivir treatment. Although V792I occurs only transiently as a passenger mutation, it is not considered a remdesivir resistance mutation because it does not confer antiviral resistance [16]. Similarly, A449V, which showed gradual increase after day 59 PI onward, has also been associated with remdesivir treatment, but also not directly with resistance. However, it has been suggested that together with the P323L mutation (consistently present at 100% frequency in all samples included) it increases the stability and activity of the RdRp complex [17], thus showing some adaptation of the virus in response to treatment. Interestingly, G671S can reduce viral replication fitness in vitro, as evidenced by slower growth and lower virus titers in Vero E6 cells [18]. This is a typical feature of drug-resistance mutations because they are often associated with fitness cost in a drugfree environment. Mutations directly linked to the use of nirmatrelvir, the main protease inhibitor encoded by the nsp5

gene, were not observed on either scale. However, mutation P132H in the nsp5 gene, which is otherwise present in over 95% of Omicron lineages (also a lineage-defining mutation of XBB.1.16.11), is associated with a reduction in thermal stability [19]. The absence of nirmatrelvir-linked mutations is most likely due to the strong conservation of the main protease active site (His41-Cys145 catalytic dyad), which limits the tolerance to functional mutations, and the high fitness cost of resistance mutations such as E166V [20]. The increase in the number of mutations after the first administration of nirmatrelvir/ritonavir (day 101) was reflected at a minor level, most prominently in the N-terminal domain (NTD) of the spike gene (Supplementary Figure S1). NTD can harbor a higher number of mutations, which may have epistatic, compensatory functions that allow prolonged infection, giving the virus more time to explore resistance pathways [21]. This observation is further supported by the fact that only prolonged treatment with a high neutralization titer CCP, more than 6.5 l over 4 months, resulted in detectable amounts of neutralizing antibodies (100 days PI), which finally cleared the viable virus between days 116 and 126 PI. Although IgG and IgA antibodies were present earlier, they did not appear to definitively affect SARSCoV-2 viability in vivo. Nevertheless, they may have played a secondary role in effector functions and immune response regulation [22]. Although neutralizing antibodies usually appear rapidly after infection [23], in cancer patients the response may be diminished in magnitude, slower to develop, less enduring, and influenced by cancer type and treatment regimens [24].

Virus culture remains the reference method for determination of virus infectivity; sgRNA markers were previously investigated as surrogates, which could offer a quick highcontainment independent way of assessing virus infectivity [25]. Our results show that neither of the sgRNAs tested correlates with culture adequately to be used as an infectivity surrogate. However, the number of human cells in the samples tested varied by approximately 3 logs, thus raising the question of sample-to-sample comparability. In addition, given the fact that the relation between gRNA and sgRNA was fairly constant during the entire course of infection, we believe that sgRNA should be further explored in a quantitative and normalized way before more accurate conclusions can be drawn.

The calculated consensus level mutation rate of 5.5×10^{-4} per site per year falls into the lower end of the established range of 10^{-3} to 10^{-4} [26]. This result may indicate a slowing down in the mutation fixation rate of Omicron compared to earlier VOCs [27]. The observed mutation rate also aligns with endemic human coronaviruses HCoV-229E and HCoV-OC43, for which an equilibrium between virus and environment has already been established [28]. In addition to replication errors, host-mediated genome editing by cell defense mechanisms can also introduce specific mutations into the SARS-CoV-2 genome. One such mechanism includes members of the APOBEC enzyme family, including APOBEC1, APOBEC3, and APOBEC3G [29]. APOBEC activity has been inferred bioinformatically by a significant excess of C→U transitions. The predominant APOBEC-associated mutation patterns, in particular the TCW→TTW transitions (W = A/T), suggest that administered antiviral treatments might be partly responsible for the occurrence of lethal mutations leading to non-viable viruses [30]. The activity of cellular antiviral proteins could in part be responsible for higher ratios of Syn and nSyn mutations, which may be a potent driver of antigenic and phenotypic changes [31]. The sustained excess of nSyn mutations suggests ongoing adaptive evolution within the host driven by positive selection pressure. Due to the patient's underlying disease and treatment, at the beginning of infection the virus is most probably under selective pressure by the antiviral treatment administered, but later on also by the host's immune response because rituximab's effect starts wearing off and the patient's immune response partially recovers. This observation underscores the potential role of chronically infected individuals as reservoirs for the emergence of evolved viral lineages due to both artificial and natural selection.

From available studies exploring relations between human microbiota and SARS-CoV-2, inconsistent results can be observed in terms of the α-diversity index, key marker organisms, and prediction of SARS-CoV-2 infection prognosis [32, 33]. In our case, the α-diversity index was lower during COVID-19 compared to the pre- and post-infection phases, which agrees with previous data [32]. We believe that the decrease in α-diversity is the result of tissue damage due to viral replication and therefore changes in the oro-/nasopharyngeal environment, which no longer supports a healthy microbiome. This allows a larger number of microorganisms, including potentially pathogenic ones, to temporarily thrive in the oro-/nasopharynx. In the case at hand, such a conclusion is supported by the observation of a higher β-diversity and detected bacterial/viral/fungal species.

Thus, we have observed that several bacterial, viral, and also fungal pathogens and opportunists can be readily detected by NGS, yet this is limited by enrichment kit selection. Moreover, some of the pathogens were detected in the upper and lower respiratory tract samples even before they were identified as the causative agents of coinfections by conventional diagnostic methods. The most likely reason for this is not the shortcomings of conventional methods per se, but the more unbiased nature of nucleic acid detection by NGS, which can find pathogens that are not yet

suspected. Such a case is clearly NGS rhinovirus detection throughout the time of SARS-CoV-2 infection. Routine diagnostics testing suggested two separate rhinovirus superinfections (93 and 147 PI) because these were the only two time points when rhinovirus testing was requested. With NGS and reads classification, we have shown that the rhinovirus coinfection was caused by a single strain that persisted throughout the time of the SARS-CoV-2 infection. Similar prolonged rhinovirus infections have been reported in healthy infants [34] and in immunocompromised patients due to transplantation [35, 36], chronic disease [37], or carcinoma [38]. Although we were unable to determine the extent to which rhinovirus is implicated in disease presentation, our study demonstrates that chronic viral coinfections should also be considered when managing such patients. We have also shown that the potential for antibiotic resistance increases with the duration of the infection; however, current metagenomic capabilities cannot yet link AMR markers to specific organisms. This limitation is also important given that the AMR markers detected were not the result of direct antibiotic treatment, but rather due to the patient's prolonged exposure to the hospital environment, where multidrug resistant strains are more prevalent [39]. This is even more pertinent during a pandemic due to the increased prescription of antibiotics to patients with SARS-CoV-2 [40]. This also appears to be the case here because the patient's bacterial coinfections were treated with two beta-lactams (meropenem and cefuroxime) and a glycopeptide (vancomycin). However, in addition to AMR genes for beta-lactams, potential resistance was observed against the MLSB group (macrolides, lincosamides, streptogramin B), aminoglycosides, and tetracyclines. These additional AMR genes most probably originated from a nosocomial source due to the patient's prolonged hospitalization, which provided ample opportunity for contact with carriers. Furthermore, the importance of the additional AMRs identified can be controversial because temporary colonization of the patient's mucosa by a commensal could also be the source.

Some limitations of the study must be acknowledged. First, the quality of nasopharyngeal swab collection cannot be standardized, which makes absolute comparisons between samples difficult. To address this to some extent, all samples were collected in equal volumes of transport medium and processed in the same way. Second, virus viability was assessed only in Vero E6 cells due to the limited quantity of samples available. Third, although all available patient sera were included in the study, a more comprehensive understanding of immune response dynamics would be possible with more samples and larger quantities, which would also allow T-cell responses to be tested. Fourth, the reproducibility of low-frequency mutations could be better assessed in independent library preparations; however, NGS sequencing would need to be performed in technical replicates for this. To mitigate this issue, we used strand bias filtering. This process checks whether the mutations detected are supported by paired sequencing reads (forward and reverse strand), thus reducing the likelihood of artificial variant calling due to strand-specific sequencing errors. Finally, the detection of coinfections and AMR markers was limited by the specificity of the hybridization probes included in the commercial NGS test. This test does not directly detect *C. krusei* or *C. albicans*, but it does detect *C. auris*.

Conclusions

In conclusion, we have demonstrated that subgenomic RNA markers, which could facilitate the determination of infectivity, are not yet well enough understood to be applicable in practice. The patient's respiratory microbiota was affected by SARS-CoV-2, and this imbalance appears to have facilitated initial coinfections. These were subsequently treated with antibiotics and antimycotics, which further disrupted the upper respiratory tract microbiome. Although AMR genes can be identified by NGS, they cannot yet be tied to specific organisms. This limitation is further demonstrated by the fact that exposure to the hospital environment over a prolonged period makes possible the acquisition of AMR markers for antibiotics that have not necessarily been used in the treatment of the patient. Our work also demonstrates that SARS-CoV-2 exhibits increased mutational activity after each antiviral treatment, seemingly in response to the artificially induced selective pressure exerted by the therapeutics administered. Taken together, this comprehensive analysis sheds more light on the complexities and pitfalls of virus clearance in individuals with hematological malignancies.

Abbreviations

AMR	antimicrobial resistance
CAR-T	chimeric antigen receptor T-cell
CCP	convalescent plasma
COVID-19	Coronavirus disease 2019
Ct	cycle threshold
gRNA	genomic RNA
NGS	next generation sequencing
nSyn	non-synonymous mutation
PI	post infection
SARS-CoV-2	Severe Acute Respiratory Syndrome Coronavirus 2
sgRNA	subgenomic RNA
Syn	synonymous mutation
Ts	transition
Tv	transversion
VOC	variant of concern

Supplementary Information

The online version contains supplementary material available at https://doi.org/10.1186/s12879-025-11355-x.

Supplementary Material 1. Detailed progression of the patient's underlying disease and treatment, and a detailed description of materials and methods are presented in the supplement.

Acknowledgements
The authors would like to express their gratitude to everyone involved in patient care and routine laboratory testing.

Authors' contributions
LB supervised and managed the clinical part of the study, collected and analyzed clinical data, and contributed to writing and reviewing the manuscript. RK was involved in NGS sample processing, comprehensive data analysis and validation, and writing and reviewing the manuscript. KRR was involved in processing samples using classical virology methods and graphic element creation, and contributed to writing the manuscript. AS and MB were involved in bioinformatic analysis, graphic element creation, and writing the manuscript. PM was involved in convalescent plasma preparation and supervision, and contributed to reviewing the manuscript. NK was involved in conceptualization of the study and contributed to the critical review of the manuscript. JT, TAŽ, and MK conceptualized the study, managed resources, supervised and administered the project, and contributed considerably to critical revision of the manuscript. MK, TAŽ, and LB were involved in funding acquisition.

Funding
This work was supported by the Slovenian Research and Innovation Agency (ARIS) under grants P3-0083, P3-0289, and J3-50101, and the Network of Infrastructure Centers of the University of Ljubljana (MRIC-UL-IC-BSL3+) under grant IP-022. The funders had no role in the design of the study; in the collection, analyses, or interpretation of data; in writing the manuscript; or in the decision to publish the results.

Data availability
The data that support the findings regarding SARS-CoV-2 of this study are openly available in GISAID's EpiCoV database, EPI_SET_241120qk, at: https://doi.org/10.55876/gis8.241120qk. Other data that support the findings of this study are available from the corresponding author upon reasonable request.

Declarations

Ethics approval and consent to participate
This study was performed in accordance with the ethical guidelines for human research, the World Medical Association's Declaration of Helsinki, the Oviedo Convention on Human Rights and Biomedicine, and the Slovenian Code of Medical Deontology. The study was approved by the Institutional Ethics Committee (ERIDNPVO-0052/2024).

Consent for publication
A written informed consent was obtained by the patient for the publication of this case report.

Competing interests
The authors declare no competing interests.

Author details
[1]Institute of Oncology Ljubljana, Ljubljana, Slovenia
[2]Institute of Microbiology and Immunology, Faculty of Medicine, University of Ljubljana, Ljubljana, Slovenia
[3]Slovenian Institute for Transfusion Medicine, Ljubljana, Slovenia
[4]Department of Infectious Diseases, University Medical Centre Ljubljana, Ljubljana, Slovenia
[5]Faculty of Medicine, University of Ljubljana, Ljubljana, Slovenia

Received: 24 April 2025 / Accepted: 9 July 2025
Published online: 21 July 2025

References

Luque-Paz D, Sesques P, Wallet F, Bachy E, Ader F. Lyon HEMINF Study Group B,-cell malignancies and COVID-19: a narrative review. Clin Microbiol Infect. 2023;29(3):332–7. https://doi.org/10.1016/j.cmi.2022.10.030.
Zannoli S, Brandolini M, Marino MM, Denicolò A, Mancini A, Taddei F, et al. SARS-CoV-2 coinfection in immunocompromised host leads to the generation of recombinant strain. Int J Infect Dis. 2023;131:65–70. https://doi.org/10.1016/j.ijid.2023.03.014.
Brandolini M, Zannoli S, Gatti G, Arfilli V, Cricca M, Dirani G, et al. Viral population heterogeneity and fluctuating mutational pattern during a persistent SARS-CoV-2 infection in an immunocompromised patient. Viruses. 2023;15(2):291. https://doi.org/10.3390/v15020291.
Leung WF, Chorlton S, Tyson J, Al-Rawahi GN, Jassem AN, Prystajecky N, et al. COVID-19 in an immunocompromised host: persistent shedding of viable SARS-CoV-2 and emergence of multiple mutations: a case report. Int J Infect Dis. 2022;114:178–82. https://doi.org/10.1016/j.ijid.2021.10.045.
Igari H, Sakao S, Ishige T, Saito K, Murata S, Yahaba M, et al. Dynamic diversity of SARS-CoV-2 genetic mutations in a lung transplantation patient with persistent COVID-19. Nat Commun. 2024;15(1):3604. https://doi.org/10.1038/s41467-024-47941-x.
Cattaneo C, Cancelli V, Imberti L, Dobbs K, Sottini A, Pagani C, et al. Production and persistence of specific antibodies in COVID-19 patients with hematologic malignancies: role of rituximab. Blood Cancer J. 2021;11(9):151. https://doi.org/10.1038/s41408-021-00546-9.
O'Nions J, Muir L, Zheng J, Rees-Spear C, Rosa A, Roustan C, et al. SARS-CoV-2 antibody responses in patients with acute leukaemia. Leukemia. 2021;35(1):289–92. https://doi.org/10.1038/s41375-020-01103-2.
Lythgoe KA, Hall M, Ferretti L, de Cesare M, MacIntyre-Cockett G, Trebes A, et al. SARS-CoV-2 within-host diversity and transmission. Science. 2021;372(6539):eabg0821. https://doi.org/10.1126/science.abg0821.
Jimenez-Araya B, Gourgeon A, N'Debi M, Thompson T, Demontant V, Simitambe A, et al. Genomics-based approach for detection and characterization of SARS-CoV-2 co-infections and diverse viral populations. Microbiol Spectr. 2025;13(6):e0209224. https://doi.org/10.1128/spectrum.02092-24.
D'Abramo A, Vita S, Nicastri E. The unmet need for COVID-19 treatment in immunocompromised patients. BMC Infect Dis. 2022;22(1):930. https://doi.org/10.1186/s12879-022-07918-x.
Focosi D, Maggi F, D'Abramo A, Nicastri E, Sullican DJ. Antiviral combination therapies for persistent COVID-19 in immunocompromised patients. Int J Infec Dis. 2023;137:55–9. https://doi.org/10.1016/j.ijid.2023.09.021.
Maria M, Maraolo AE, Cozzolino C, Sasset L, Ferrari A, Basso M, et al. Does early combination vs. monotherapy improve clinical outcomes of clinically extremely vulnerable patients with COVID-19? Results from a retrospective propensity-weighted analysis. Eur J Med Res. 2024;29(1):484. https://doi.org/10.1186/s40001-024-02062-5.
Mendes-Correa MC, Salomão MC, Ghilardi F, Tozetto-Mendoza TR, Santos Villas-Boas L, et al. SARS-CoV-2 Detection and culture in different biological specimens from immunocompetent and immunosuppressed COVID-19 patients infected with two different viral strains. Viruses. 2023;15(6):1270. https://doi.org/10.3390/v15061270.
Wölfel R, Corman VM, Guggemos W, Seilmaier M, Zange S, Müller MA, et al. Virological assessment of hospitalized patients with COVID-2019. Nature. 2020;581(7809):465–9. https://doi.org/10.1038/s41586-020-2196-x.
Sissoko D, Duraffour S, Kerber R, Kolie JS, Beavogui AH, Camara AM, et al. Persistence and clearance of Ebola virus RNA from seminal fluid of Ebola virus disease survivors: a longitudinal analysis and modelling study. Lancet Glob Health. 2017;5(1):e80-8. https://doi.org/10.1016/S2214-109X(16)30243-1.
Yang S, Multani A, Garrigues JM, Oh MS, Hemarajata P, Burleson T, et al. Transient SARS-CoV-2 RNA-dependent RNA polymerase mutations after remdesivir treatment for chronic COVID-19 in two transplant recipients: case report and intra-host viral genomic investigation. Microorganisms. 2023;11(8):2096. https://doi.org/10.3390/microorganisms11082096.
Ling-Hu T, Simons LM, Rios-Guzman E, Carvalho AM, Agnes MFR, Alisoltanidehkordi A, et al. The impact of remdesivir on SARS-CoV-2 evolution in vivo. JCI Insight. 2025;10(4). https://doi.org/10.1172/jci.insight.182376.
Stevens LJ, Pruijssers AJ, Lee HW, Gordon CJ, Tchesnokov EP, Gribble J, et al. Mutations in the SARS-CoV-2 RNA-dependent RNA polymerase confer resistance to remdesivir by distinct mechanisms. Sci Transl Med. 2022;14(656):eabo0718. https://doi.org/10.1126/scitranslmed.abo0718.
Sacco MD, Hu Y, Gongora MV, Meilleur F, Kemp MT, Zhang X, et al. The P132H mutation in the main protease of Omicron SARS-CoV-2 decreases thermal

stability without compromising catalysis or small-molecule drug inhibition. Cell Res. 2022;32(5):498–500. https://doi.org/10.1038/s41422-022-00640-y.
Iketani S, Mohri H, Culbertson B, Hong SJ, Duan Y, Luck MI, et al. Multiple pathways for SARS-CoV-2 resistance to nirmatrelvir. Nature. 2023;613(7944):558–64. https://doi.org/10.1038/s41586-022-05514-2.
Witte L, Baharani VA, Schmidt F, Wang Z, Cho A, Raspe R, et al. Epistasis lowers the genetic barrier to SARS-CoV-2 neutralizing antibody escape. Nat Commun. 2023;14(1):302. https://doi.org/10.1038/s41467-023-35927-0.
Reinig S, Shih SR. Non-neutralizing functions in anti-SARS-CoV-2 IgG antibodies. Biomed J. 2024;47(1). https://doi.org/10.1016/j.bj.2023.100666.
Muecksch F, Wise H, Batchelor B, Squires M, Semple E, Richardson C, et al. Longitudinal serological analysis and neutralizing antibody levels in coronavirus disease 2019 convalescent patients. J Infect Dis. 2021;223(3):389–98. https://doi.org/10.1093/infdis/jiaa659.
Zeng C, Evans JP, Reisinger S, Woyach J, Liscynesky C, Boghdadly ZE, et al. Impaired neutralizing antibody response to COVID-19 mRNA vaccines in cancer patients. Cell Biosci. 2021;11(1):197. https://doi.org/10.1186/s13578-021-00713-2.
Verma R, Kim E, Martínez-Colón GJ, Jagannathan P, Rustagi A, Parsonnet J, et al. SARS-CoV-2 subgenomic RNA kinetics in longitudinal clinical samples. Open Forum Infect Dis. 2021;8(7):ofab310. https://doi.org/10.1093/ofid/ofab310.
González-Vázquez LD, Arenas M. Molecular evolution of SARS-CoV-2 during the COVID-19 pandemic. Genes (Basel). 2023;14(2):407. https://doi.org/10.3390/genes14020407.
Alquraan L, Alzoubi KH, Rababa'h SY. Mutations of SARS-CoV-2 and their impact on disease diagnosis and severity. Inform Med Unlocked. 2023;39. https://doi.org/10.1016/j.imu.2023.101256.
Jo WK, Drosten C, Drexler JF. The evolutionary dynamics of endemic human coronaviruses. Virus Evol. 2021;7(1):veab020. https://doi.org/10.1093/ve/veab020.
Kim K, Calabrese P, Wang S, Qin C, Rao Y, Feng P, et al. The roles of APOBEC-mediated RNA editing in SARS-CoV-2 mutations, replication and fitness. Sci Rep. 2022;12(1):14972. https://doi.org/10.1038/s41598-022-19067-x.
Wang S, Jia M, He Z, Liu XS. APOBEC3B and APOBEC mutational signature as potential predictive markers for immunotherapy response in non-small cell lung cancer. Oncogene. 2018;37(29):3924–36. https://doi.org/10.1038/s41388-018-0245-9.
31. Simmonds P. Rampant C→U hypermutation in the genomes of SARS-CoV-2 and other coronaviruses: causes and consequences for their short- and long-term evolutionary trajectories. mSphere. 2020;5(3):e00408-20. https://doi.org/10.1128/mSphere.00408-20.
Xu R, Liu P, Zhang T, Wu Q, Zeng M, Ma Y, et al. Progressive deterioration of the upper respiratory tract and the gut microbiomes in children during the early infection stages of COVID-19. J Genet Genomics. 2021;48(9):803–14. https://doi.org/10.1016/j.jgg.2021.05.004.
Hurst JH, McCumber AW, Aquino JN, Rodriguez J, Heston SM, Lugo DJ, et al. Age-related changes in the nasopharyngeal microbiome are associated with severe acute respiratory syndrome coronavirus 2 (SARS-CoV-2) infection and symptoms among children, adolescents, and young adults. Clin Infect Dis. 2022;75(1):e928-37. https://doi.org/10.1093/cid/ciac184.
Loeffelholz MJ, Trujillo R, Pyles RB, Miller AL, Alvarez-Fernandez P, Pong DL, et al. Duration of rhinovirus shedding in the upper respiratory tract in the first year of life. Pediatrics. 2014;134(6):1144–50. https://doi.org/10.1542/peds.2014-2132.
Kaiser L, Aubert JD, Pache JC, Deffernez C, Rochat T, Garbino J, et al. Chronic rhinoviral infection in lung transplant recipients. Am J Respir Crit Care Med. 2006;174(12):1392–9. https://doi.org/10.1164/rccm.200604-489OC.
Piralla A, Zecca M, Comoli P, Girello A, Maccario R, Baldanti F. Persistent rhinovirus infection in pediatric hematopoietic stem cell transplant recipients with impaired cellular immunity. J Clin Virol. 2015;67:38–42. https://doi.org/10.1016/j.jcv.2015.03.022.
Flight WG, Bright-Thomas RJ, Tilston P, Mutton KJ, Guiver M, Webb AK, et al. Chronic rhinovirus infection in an adult with cystic fibrosis. J Clin Microbiol. 2013;51(11):3893–6. https://doi.org/10.1128/JCM.01604-13.
Dysangco AT, Kressel AB, Dearth SM, Patel RP, Richards SM. Prolonged rhinovirus shedding in a patient with Hodgkin disease. Infect Control Hosp Epidemiol. 2017;38(4):500–1. https://doi.org/10.1017/ice.2016.338.
Flynn CE, Guarner J. Emerging antimicrobial resistance. Mod Pathol. 2023;36(9). https://doi.org/10.1016/j.modpat.2023.100249.
Nandi A, Pecetta S, Bloom DE. Global antibiotic use during the COVID-19 pandemic analysis of pharmaceutical sales data from 71 countries 2020–2022. Clin Med. 2023;57. https://doi.org/10.1016/j.eclinm.2023.101848.

Publisher's note